Clay Products Convective Drying: Foundations, Modeling and Applications

A.G. Barbosa de Lima, J. Barbosa da Silva, G.S. Almeida, J.J.S. Nascimento, F.V.S. Tavares and V.S. Silva

Abstract This chapter briefly focuses on the theory and applications of drying process with particular reference to wet clay product. Herein, a modeling based on the heat and liquid diffusion theories including dimensions variations and hygro-thermal-elastic stress analysis, and the mathematical formalism to obtain the numerical solution of the governing equations using finite-volume method are presented. The model considers constant thermo-physical properties and convective boundary conditions at the surface of the solid. Applications have been done to ceramic hollow brick. Predicted results of the average moisture content, surface temperature, and moisture content, temperature and stress distributions within the porous solids are shown and analyzed, and for some drying situations they are compared with experimental drying data of the average moisture content and surface temperature of the brick along the continuous drying process.

A.G. Barbosa de Lima (✉) · J.B. da Silva · F.V.S. Tavares · V.S. Silva
Department of Mechanical Engineering, Federal University of Campina Grande, Av. Aprígio Veloso, 882, Bodocongó, 58429-900 Campina Grande, PB, Brazil
e-mail: antonio.gilson@ufcg.edu.br

J.B. da Silva
e-mail: barbosa.joselito@gmail.com

F.V.S. Tavares
e-mail: valdeiza.tavares@hotmail.com

V.S. Silva
e-mail: veralucia.silva84@yahoo.com.br

G.S. Almeida
Federal Institute of Education, Science and Technology of Roraima, IFRR, Boa Vista-RR, Brazil
e-mail: genival.almeida@ifrr.edu.br

J.J.S. Nascimento
Department of Materials Engineering, Federal University of Campina Grande, Av. Aprígio Veloso, 882, Bodocongó, Campina Grande, PB 58429-900, Brazil
e-mail: jefferson@dema.ufcg.edu.br

J.M.P.Q. Delgado and A.G. Barbosa de Lima (eds.),
Drying and Energy Technologies, Advanced Structured Materials 63,
DOI 10.1007/978-3-319-19767-8_3

Keywords Drying · Numerical · Experimental · Hollow brick

1 Introduction

Ceramic processing has traditionally been discussed in term of the material formulation and industrial arts used in the production of commercial products that are very different in size, shape, detail, complexity, material composition, structure, and cost. Structural clay products include e.g. building bricks and tiles (traditional ceramics) where in which structural intensity is very important [1, 2]. One important concern in the application of ceramic materials is the fabrication technique. Clay minerals, when mixed with water, become highly plastic (hydroplasticity) and it can be molded at different shapes easily without cracking. These physical and chemical characteristics maintain the body shape during handling, drying and firing. The water added to ceramic clay cover the surface of the clay particle (forming a thin film around the clay particles), fills small capillaries and porous, and causes a separation of particles inside it [3]. Then, the particles are free to moving over another resulting in plasticity of the water-clay system.

After plastic forming and casting, products must be dried, in order, to removal of the moisture prior for further processing and/or firing. If this moisture is not entirely removed, the extreme temperature in the kiln will force out this water during firing, causing cracking and until explosion of the product. In the case of argils, to promote an understanding of the drying mechanism, a microscopic investigation in the state of the moisture inside the product it is requested [4–6].

In this sense, some authors they affirm that during clay drying, the dominant mechanism of moisture migration is the liquid transport [7–12], while another they consider that exist liquid and vapor transport inside the solid [13–15]. On the basis of their hypothesis several studies on clay drying have been reported in the literature [16–26].

Drying is a simultaneous of heat and mass transfer including dimension variations. As drying progresses and water is removed, the interparticle separation decreases, a condition termed shrinkage [1, 2]. During the drying of ceramics products, heat is transported to the liquid inside the solid, and simultaneously moisture is transported to out of solid, generating dilation by heating and contraction by moisture removal.

Drying of ceramics is accomplished by evaporation of water. If the rate of liquid water evaporation at the surface of the clay body is greater than the rate of liquid water diffusion inside the solid, the surface will dry more quickly than the interior by causing stresses and probable defects or perhaps revealing them.

These mechanisms of heat and mass transfer are more intense in ceramic materials with high initial moisture content, mainly in products of fine granulation and gives rise to hygro-thermal stresses on the product. The magnitude of these

stresses will depend on the shape, thermo-physical and elastic properties, and contraction and expansion coefficients of the material.

Different factors like area/volume relationships, initial water content, granulometry (clay particle size) and shape of the formed body, and air-drying conditions (temperature, relative humidity and flow rate) affect shrinkage phenomenon. Then, it is critical to control the rate of water removal during clay materials drying [4–6]. These defects range from visible defects (such as cracks) to a reduction in physical properties in fired clay products in areas such as strength, elastic modulus, color and appearance (discoloration due to summing) [3]. Beside, drying represents a process cost to the manufacturer in terms of handling and in terms of energy costs to accomplish drying. Then, deformation and failure of clay drying are great problems in a ceramic production. Therefore the stress control during drying process is relevant for the quality of the product after drying and for energy saving.

2 Clay Drying

2.1 Foundations

Brick is a commercial ceramic product made of clay minerals and has been used in worldwide for centuries in house wall and building constructions. The ceramic product, during the manufacturing process, goes through the steps of product shaping (molding), drying and firing [1–3]. The drying is the phase of the process that precedes firing and needs an appreciable amount of thermal energy to evaporate the water which was added during the molding process [1, 6]. The purpose of this step is to reduce slowly and uniformly, the moisture of the products from 20–25 %, after extrusion or pressing, to 3–10 % at the end of drying. Drying causes shrinkage of product which can vary, in general, from 4 to 10 %. In case of the ceramic products, where red clay is used, the drying stage has a great importance. In this step most of the water contained in the product is eliminated. Consequently higher shrinkage and dilation of material results and the product often gets rejected due to its low quality. The published [3, 6] literature shows that if a special care is taken during the drying step energy cost can be reduced and a better quality product can be obtained.

When the ceramic product drying operation is natural, the pieces are stacked in covered sheds, arranged on shelves (fixed or mobile) or simply piled on the floor. The duration of drying depends on the material characteristics and state conditions of atmospheric air (temperature and relative humidity) and of the ventilation of the place, needing periods of up to 6 weeks. However, to reduce drying time, artificial drying is carried out in drying chambers or ovens, using, as a rule, the residual heat of the furnaces, while these are being cooled. The most common types of artificial dryers are static, continuous or semi continuous. The period of artificial drying depends on the characteristics of the raw material, the shape of the pieces to be

dried and the type of dryer and air drying conditions. It has an average variation of 12–40 h. Artificial drying is carried out at temperature 80–110 °C, and precise information about the relative humidity are practically non-existent in the literature, though it can be said that this is very high [5, 27].

The choice of a particular type of dryer for a particular drying operation is a complex task by virtue of the existence of many factors that affect the selection. In particular, factors to be considered during the drying process includes the drying technique, heating method and the mass and energy exchanges mechanisms between the product and the drying air. Currently certain preference is given to tunnel and batch (type oven) dryers for drying of ceramic materials, specifically red ceramic one. Within this context, for the purpose of searching new technologies for the sector, improvement of the product quality and rationalization of energy consumption, several studies have been conducted [12, 28–32].

Because of the importance and cost of the drying procedure, mainly in industrial scale mathematical models to describe the drying process of ceramic material have been reported by many researchers [6, 7, 9, 10, 12–15, 24, 33–41].

Depending on the thickness of the material studied, these models can be classified into: drying in a thin layer (particle models) and drying in a thick layer (dryer level models). The drying of a single particle individually or even of a layer of material of small thickness, does not modify the drying conditions significantly as the air past over the wet porous solid. The practical importance of thin layer drying is very limited, because the materials are generally dried in thick layers: stationary or moving. When the material is placed inside of a dryer, forming a thick layer, the thermodynamic properties of the drying air are modified markedly as the air flows through it. In virtue of this, the models of drying in thick layer, having more complex equations that take into account the heat and mass transfer between the product and the surrounding air, are more complete than the thin layer drying model.

Despite of the importance on the dryer model in the chapter special attention should be done to a robust particle model with particular reference to industrial hollow brick drying.

2.2 Mathematical Modeling: Application to Hollow Brick

Drying characteristics of the particular materials being dried and simulation models are needed in the design, construction and operation of drying systems. Several empirical, semi-empirical, and theoretical models have been proposed to predict drying process of different materials. For convective drying process, theoretical models take into account both internal and external resistance while the semi-empirical and empirical models (lumped models) take into account only external resistance to heat and moisture transfer between porous solid and air surrounding it (internal resistance is negligible). At present, there are very few models that represent the batch drying of clay products specially brick. As

shrinkage in clay brick is an observable phenomenon during drying process and may have significant effect on mass diffusivity, it must be taken into account in order to obtain reliable predictions of performance. Despite of the importance, because the simplifications, the lumped models cannot give clear and accurate of the fundamentals of the drying process, but they can used to complete mathematical models at the level of the drying equipment.

Mass transfer during falling rate period is caused by liquid diffusion or capillary flow. The former is commonly used to describe drying behavior in the falling rate period of clay products. In the liquid diffusion theory [42–44], the rate of diffusion is governed by moisture concentration gradient as the driving force. Fick's law of diffusion is widely used to model the drying behavior for this period.

Heat flux inside the wet clay porous product during drying process can be modeled by considering heat conduction as unique mechanism of heat transfer. In this case we can use the Fourier´s law to model this heating process.

To describe the liquid and heat transfer inside the clay brick, the following assumptions were used:

- The thermo-physical properties are constant, during the whole drying process;
- Source term of energy and mass is neglected;
- The solid is homogeneous and isotropic;
- The moisture content and temperature distributions are uniform at the beginning of the process;
- The phenomenon happens under convective condition at the surface of the body.
- The shrinkage of the solid is polynomial function of the moisture content;
- The solid is composed of water in liquid phase and solid material.
- The diffusion phenomenon occurs under falling rate.

Figure 1 illustrates a solid parallelepiped of dimensions $2R_1 \times 2R_2 \times 2R_3$. For this case, the general partial differential equations that describe the unsteady diffusion phenomenon in a three-dimensional situation it is in the way as follows

2.2.1 Mass Transfer Model

For mass transfer in the absence of mass source, the Fick´s law was used as follows:

$$\frac{\partial M}{\partial t} = \nabla \cdot (D \nabla M) \tag{1}$$

where M (moisture content, dry basis), D represents mass diffusion coefficient and t is the time.

Due to the symmetry in the solid, in the planes (x = 0, y, z), (x, y = 0, z), (x, y, z = 0) it was considered 1/8 of the total volume of the solid. Therefore, the initial, symmetry and boundary conditions are as follows:

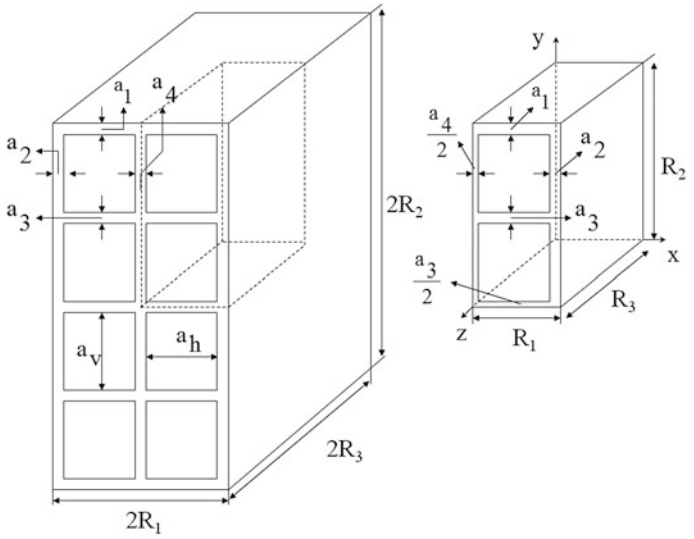

Fig. 1 Geometrical parameters of a specific hollow brick

- Initial condition:

$$\mathrm{M}(\mathrm{x},\ \mathrm{y},\ \mathrm{z},\ \mathrm{t}=0)=\mathrm{M_o} \tag{2}$$

- Symmetry condition:

$$\frac{\partial \mathrm{M}(\mathrm{x}=0,\mathrm{y},\ \mathrm{z},\ \mathrm{t})}{\partial \mathrm{x}}=\frac{\partial \mathrm{M}(\mathrm{x},\ \mathrm{y}=0,\mathrm{z},\ \mathrm{t})}{\partial \mathrm{y}}=\frac{\partial \mathrm{M}(\mathrm{x},\ \mathrm{y},\ \mathrm{z}=0,\mathrm{t})}{\partial \mathrm{z}}=0,\ \ \mathrm{t}>0 \tag{3}$$

- Boundary condition:

$$-D\frac{\partial \mathrm{M}(\mathrm{x}=R_1,\mathrm{y},\ \mathrm{z},\ \mathrm{t})}{\partial \mathrm{x}}=h_m[\mathrm{M}(\mathrm{x}=R_1,\mathrm{y},\ \mathrm{z},\ \mathrm{t})-M_e] \tag{4}$$

$$-D\frac{\partial \mathrm{M}(\mathrm{x},\ \mathrm{y}=R_2,\mathrm{z},\ \mathrm{t})}{\partial \mathrm{y}}=h_m[\mathrm{M}(\mathrm{x},\ \mathrm{y}=R_2,\mathrm{z},\ \mathrm{t})-\mathrm{M}_e] \tag{5}$$

$$-D\frac{\partial \mathrm{M}(\mathrm{x},\ \mathrm{y},\ \mathrm{z}=R_3,t)}{\partial \mathrm{z}}=h_m[\mathrm{M}(\mathrm{x},\ \mathrm{y},\ \mathrm{z}=R_3,t)-\mathrm{M}_e] \tag{6}$$

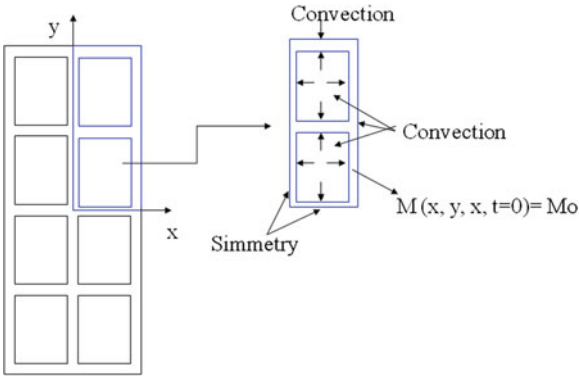

Fig. 2 Scheme showing the boundary conditions in the hollow brick

where h_m correspond to convective mass transfer coefficient and M_e represents equilibrium moisture content of the porous solid with the drying air.

For convenience, Fig. 2 illustrates better the initial, symmetry and boundary conditions.

2.2.2 Heat Transfer Model

For heat transfer, in the absence of energy source term, the Fourier´s law was used as follows:

$$\frac{\partial \theta}{\partial t} = \nabla \cdot (\alpha \nabla \theta) \tag{7}$$

where θ is the solid temperature and $\alpha = k/(\rho c_p)$ represent thermal diffusivity, being k the thermal conductivity, c_p the specific heat and ρ is the solid density.

The initial, symmetry and boundary conditions are as follows:

- Initial condition:

$$\theta(x, y, z, t = 0) = \theta_o \tag{8}$$

- Symmetry condition:

$$\frac{\partial \theta(x = 0, y, z, t)}{\partial x} = \frac{\partial \theta(x, y = 0, z, t)}{\partial y} = \frac{\partial \theta(x, y, z = 0, t)}{\partial z} = 0, \; t > 0 \tag{9}$$

- Boundary condition:

$$-\mathrm{k}\frac{\partial\theta(\mathrm{x}=\mathrm{R}_1,\mathrm{y},\mathrm{z},\mathrm{t})}{\partial\mathrm{x}}=h_c[\theta(\mathrm{x}=\mathrm{R}_1,\mathrm{y},\mathrm{z},\mathrm{t})-\theta_e] \tag{10}$$

$$-\mathrm{k}\frac{\partial\theta(\mathrm{x},\mathrm{y}=\mathrm{R}_2,\mathrm{z},\mathrm{t})}{\partial\mathrm{y}}=h_c[\theta(\mathrm{x},\mathrm{y}=\mathrm{R}_2,\mathrm{z},\mathrm{t})-\theta_e] \tag{11}$$

$$-\mathrm{k}\frac{\partial\theta(\mathrm{x},\mathrm{y},\mathrm{z}=\mathrm{R}_3,t)}{\partial\mathrm{z}}=h_c[\theta(\mathrm{x},\mathrm{y},\mathrm{z}=\mathrm{R}_3,\mathrm{t})-\theta_e] \tag{12}$$

where h_c correspond to convective heat transfer coefficient and θ_e represents equilibrium temperature between the solid and drying air.

The average value of moisture content or temperature was obtained as follows:

$$\bar{\Phi}=\int_{\mathrm{v}}\Phi\mathrm{dV} \tag{13}$$

where $\Phi = \theta$ (temperature) or $\Phi = \mathrm{M}$ (moisture content, dry basis) and V is the volume of the solid.

2.2.3 Volume Variations Model

During drying process, the wet porous solid surfer expansion (dilation) by heating and contraction (shrinkage) by loss of water. Dilation phenomenon has few effect on the dimension variation of the solid because the volumetric dilation coefficient is smallest than the shrinkage coefficient. Thus, following equation was utilized to obtain the changes in volume (shrinkage) in each time during the drying process:

$$\mathrm{V_t}=\mathrm{V_o}\left(\mathrm{b_1}\overline{\mathrm{M}}^3+\mathrm{b_2}\overline{\mathrm{M}}^2+\mathrm{b_3}\overline{\mathrm{M}}+\mathrm{b_4}\right) \tag{14}$$

where V_o is initial volume of the brick and b_1, b_2, b_3 and b_4 are parameters to be determined by fitting to experimental data.

The volume of the hollow brick is given by:

$$(\mathrm{V})_\mathrm{t}=8[\mathrm{R_1R_2R_3}-2\mathrm{a_v a_h R_3}] \tag{15}$$

where $a_v = [2R_2 - (2a_1 + 3a_3)]/4$ and $a_h = [2R_1 - (2a_2 + a_4)]/2$.

The surface area of heat and mass transfer of the solid during the drying process was obtained by:

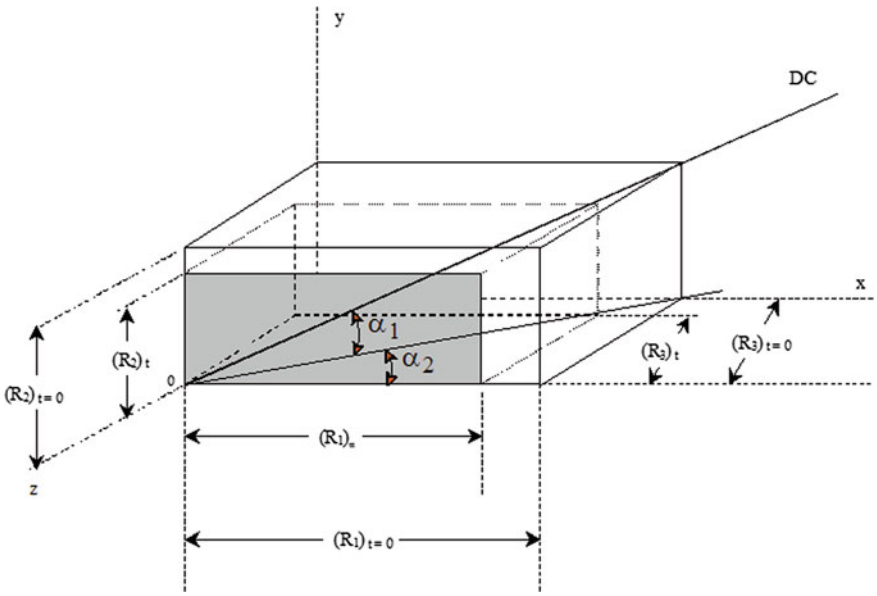

Fig. 3 Shrinkage of a solid parallelepiped during the drying process

$$A_s = 8[R_1R_2 + R_2R_3 + R_1R_3 - 2a_v a_h + 4a_v R_3 + 4a_h R_3] \tag{16}$$

For the calculation of the new volume and surface area of the brick during drying process considers the Fig. 3. Based on this figure was assumed an isotropic shrinkage. Thus, is possible to demonstrate that:

$$\tan \alpha_2 = \frac{(R_3)_t}{(R_1)_t} = \frac{(R_3)_{t=0}}{(R_1)_{t-0}} = \hat{k}1 \tag{17}$$

$$\tan \alpha_1 = \frac{(R_2)_t}{\sqrt{(R_1)_t^2 + (R_3)_t^2}} = \frac{(R_2)_{t=0}}{\sqrt{(R_1)_{t=0}^2 + (R_3)_{t=0}^2}} = \hat{k}2 \tag{18}$$

where $\hat{k}1$ and $\hat{k}2$ are constant. So by combining Eqs. (14), (17) and (18) the new dimension of the porous body can be determined in each instant of the drying process.

2.2.4 Stress Model

The governing equation in a stress field derived from force balance for static equilibrium can be expressed as follows:

$$\nabla\sigma + \vec{F} = 0 \tag{19}$$

where σ is a stress tensor and $\vec{F}$ is a body force vector.

At the surface, the boundary conditions can be described as follows:

$$u = u_a \text{ and } \sigma \cdot \vec{n} = t \tag{20}$$

where u_a is a prescribed displacement and t is a traction on the boundary.

The basic assumption of a constitutive model in a stress field is that a strain tensor represents the sum of the strains caused by traction, temperature and moisture as follows:

$$e = \frac{1}{E}(\sigma - \sigma_o) + \gamma\Delta\theta + \beta\Delta M \tag{21}$$

where e is a total mechanical strain tensor, σ is a total stress tensor, σ_o is an initial stress tensor, E is an elastic coefficient, γ is a thermal expansion coefficient, $\Delta\theta = \theta - \theta_o$ is a temperature variation, β is a moisture expansion coefficient (effective shrinkage coefficient) and $\Delta M = M - M_o$ is a moisture content variation. Stresses caused by thermal expansion (heating) are opposed those caused by drying shrinkage (moisture removal).

In a hygro-thermal stress problem, the thermal and moisture effects may be treated as that of an initial stress. The constitutive equation based in the Eq. (21) can be defined as follows [45–47].

$$\sigma = E(e - \gamma\Delta\theta - 0\Delta M) + \sigma_o = Ee + \sigma'_o \tag{22}$$

According to elasticity theory [48], there are three principal stresses formed at any location in a strained body (Fig. 4). These stresses are oriented orthogonally to each other, and unidirectional stresses (tensile or compressive stresses) are locally maximum along these orientations [49]. Based on this theory, the following assumptions were adopted:

- No initial stress σ_o are applied to the brick;
- Mechanical strain are neglected ($\varepsilon_x = \varepsilon_y = \varepsilon_z = e = 0$);
- Internal stresses (σ_x, σ_y and σ_z) are due to hygro and thermal strains due to dilation and shrinkage;
- Hygro and thermal strain causes expansion and contraction and the change volume element. No shear exists. This way the shape of the element is unchanged. The body is unrestrained (free to expand and constrains).
- Because no shear stress occurs, the stresses (σ_x, σ_y and σ_z) are the principal stresses (maximum normal stress in each location in the brick).

According to these considerations, the total stress inside the brick is the sum of hygro and thermal stresses. So, by using Eq. (22), the normal stress in the x, y and z directions can be calculated using the following equations:

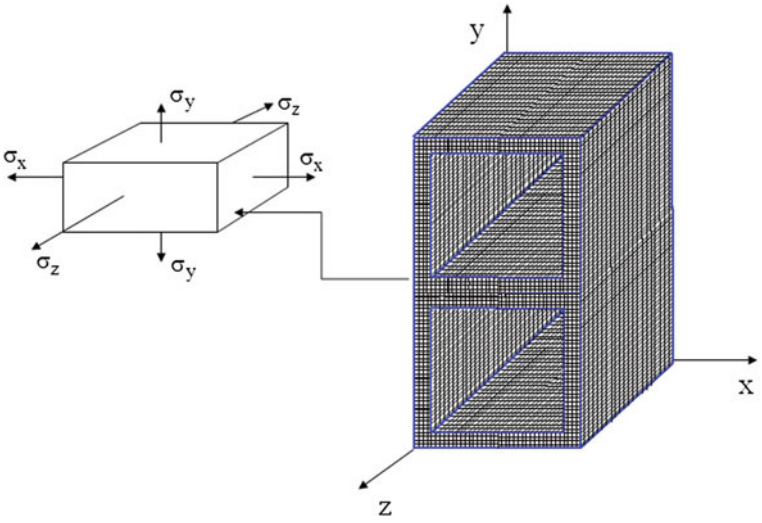

Fig. 4 Principal stresses σ_x, σ_y, and σ_z applied in a location inside the brick

$$(-\alpha_{\theta x}\Delta\theta - \alpha_{Mx}\Delta M)E = [\sigma_x - \nu(\sigma_y + \sigma_z)] \tag{23}$$

$$(-\alpha_{\theta y}\Delta\theta - \alpha_{My}\Delta M)E = [\sigma_y - \nu(\sigma_x + \sigma_z)] \tag{24}$$

$$(-\alpha_{\theta z}\Delta\theta - \alpha_{Mz}\Delta M)E = [\sigma_z - \nu(\sigma_x + \sigma_y)] \tag{25}$$

where ν is the Poisson coefficient, $\alpha_{\theta x} = \alpha_{\theta y} = \alpha_{\theta z} = \alpha_\theta$ are the linear thermal expansion coefficients and $\alpha_{Mx} = \alpha_{My} = \alpha_{Mz} = \alpha_M$ are the linear hydrical expansion coefficients. Solving the linear equation system (Eqs. 23–25) σ_x, σ_y and σ_z can be determined as follows:

$$\sigma_x = \sigma_y = \frac{[(-\alpha_\theta\Delta\theta - \alpha_M\Delta M)E + \nu\sigma_z]}{1 - \nu} \tag{26}$$

$$\sigma_z = \frac{2E(-\alpha_\theta\Delta\theta - \alpha_M\Delta M)}{(2\nu - 1)} \tag{27}$$

2.3 Numerical Solution

Literature reports different exact (separation of variables, Laplace Transform, Galerkin-based integral method, etc.) and numerical (finite difference, finite element, boundary element, finite volume, etc.) methods to solve a partial differential equation. In this chapter was used the finite-volume method to discretize the basic

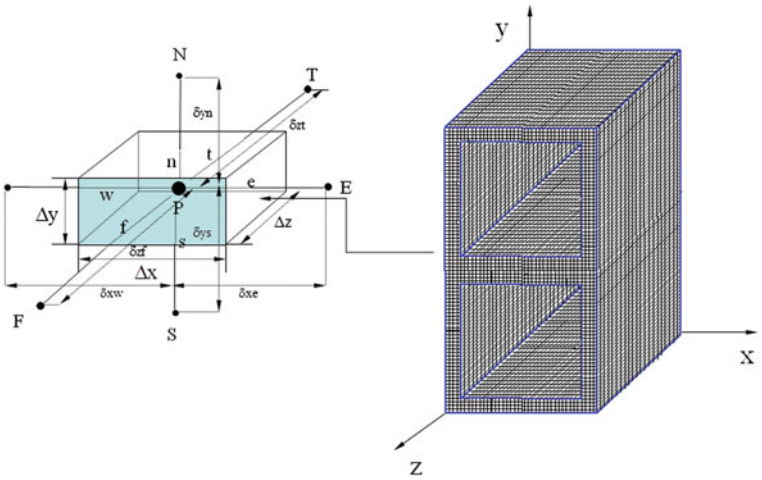

Fig. 5 Control-volume and grid used in this work

equations. Now a three-dimensional grid is used to subdivide the domain. The cell contain node P and six neighboring nodes identified as west, east, south, north, bottom and top nodes. Figure 5 represents the differential volume of the physical domain (Fig. 1), where the nodal points (W, E, N, S, F, T) and geometrical parameters of the control volume are presented.

Assuming fully implicit scheme, where all terms are estimated in t + Δt, the Eqs. (1) and (7) were integrated in the control volume of the Fig. 5, that correspond to the internal points of the domain, and also in the time. As results of this mathematical procedure the following discretization equation [50–52] in the short form was obtained:

$$A_P\Phi_P = A_E\Phi_E + A_W\Phi_W + A_N\Phi_N + A_S\Phi_S + A_T\Phi_T + A_F\Phi_F + B \tag{28}$$

The implicit method is recommended for general purpose transient calculations because of its robustness and unconditional stability. Discretized equation must be set up at each of the nodal points in order to solve a problem. Starting with initial field for the potential Φ (mass or temperature) applied to all nodes the set of equations is solved iteratively until a converged solution is obtained. Here the set of equations are solved iteratively using the Gauss-Seidel method. The following convergence criterion was used.

$$\left|\Phi^{n+1} - \Phi^{n}\right| \leq 10^{-8} \tag{29}$$

where n represents the n-th iteration in each time. Details about the numerical procedure can be found in [9–11, 23, 27].

2.4 Experimental Study of Hollow Brick

For the drying experiment, industrial hollow brick (clay) was dried in an oven under controlled conditions of air (velocity, temperature and relative humidity). The geometrical parameters and initial conditions of the material are show in the Table 1. The sample was weighed and measured dimensions and surface temperature at 10 min intervals during the drying process. Figure 6 illustrates a scheme of the clay brick used in this work indicating the point where surface temperature was measured. The continuous drying experiments ended when the mass reached constant weight. In order, to obtain the balanced moisture content, the sample was kept under the same temperature for 48 h inside the oven. The test was performed under atmospheric pressure. Details about the experimental procedure can be found in [23, 25].

2.5 Results Analysis

2.5.1 Experimental

The collected data of the chemical analyses of clay used for brick molding are show in the Table 2. There data suggest that the clay of the Brazilian region is basically rich in aluminum (Al_2O_3), Silica (SiO_2), and iron oxide (Fe_2O_3).

In order to analyze the effects of drying air conditions on the moisture removal and heating of ceramic bricks, experimental data of the dimensionless average moisture content, dimensionless surface temperature (vertex) and volume variations of the brick obtained during the drying were plotted for two drying conditions as seen in the Figs. 7, 8, 9, 10, 11 and 12.

By comparing the data, one could see that the drying air temperature has influenced strongly the drying rate as expected. When the temperature increases, so does the drying rate increase too. However, this may give rise to high temperatures and thermal and hydric gradients into the solid, which would induce thermal, hydrical and mechanical stresses (Figs. 10, 11, 12 and 13). The highest moisture content and temperature gradients occur at the surface of the solid mainly close to the vertexes of the solid, rendering theses regions more vulnerable to cracks and fissures. It can be seen that the stresses have produced serious cracks, fissures and deformations in the brick contributing, as a result, towards a decrease in the quality of the solid at the end of drying process. The mechanical behavior of clay is generally described as elastic viscosity and plasticity depending on the moisture content. Further, the drying rate can also be affected by the shape of the brick and air relative humidity. For higher area/volume relationships and lower air relative humidity we have, as expected, higher drying and shrinkage velocities. It was observed that the y-axis shrink more than x-axis due to the fact of $R_2 > R_1$. The shrinkage is proportional the dimensions of the solid, so, different deformations and

Table 1 Experimental parameters of the clay brick and drying-air

Air			Holed clay brick											
RH (%)	T (°C)	v (m/s)	$2R_1$ (mm)	$2R_2$ (mm)	$2R_3$ (mm)	a_1 (mm)	a_2 (mm)	a_3 (mm)	a_4 (mm)	M_o (d.b.)[a]	M_e (d.b.)	θ_0 (°C)	θ_f (°C)	t (h)
4.6	80.0	1.0	92.76	197.0	201.0	8.16	7.20	7.84	6.66	0.152	0.00039	21.4	69.2	15.0
1.8	100.0	1.0	92.80	198.0	202.0	11.70	9.41	8.74	8.00	0.169	0.00038	26.1	93.2	12.3

[a]d.b. (dry basis)—kg water/kg dry solid

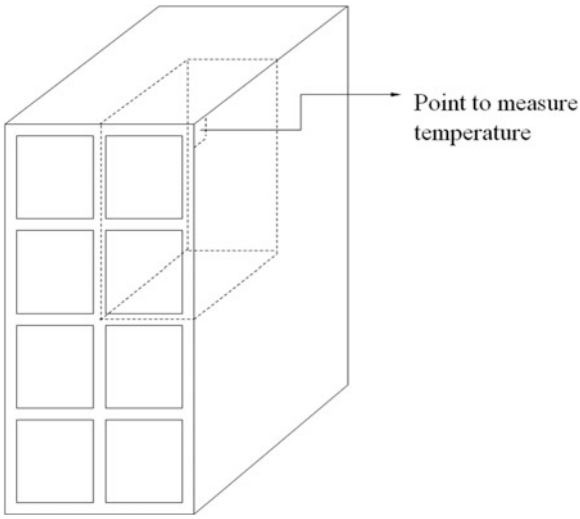

Fig. 6 The geometry of industrial brick

shrinkage velocity occurs in the x, y and z directions. According to Figs. 9 and 10 can be verified that shrinkage is not linear and become more intense as increasing air temperature. Volume variations closed to 13 and 22 %, were obtained close to for temperatures 80 and 100 °C, respectively.

2.5.2 Simulations

As purpose to evaluate the robustness of the mathematical modeling presented before, this one was used to predict hollow brick drying process. Simulations were performed using a grid with 20 × 20 × 20 nodal points and $\Delta t = 1$ s. These conditions were obtained by successive grid and time step refinements. The following data were used: $D = 8.0 \times 10^{-10}$ m^2/s; $\alpha = k/\rho c_p = 1.0 \times 10^{-7}$ m^2/s; $h_m = 1.0 \times 10^{30}$ m/s; $h_c = 2.41$ W/m^2 K; $\alpha_M = \beta/3 = 3.3 \times 10^{-2}$; $\alpha_\theta = \gamma/3 = 6.0 \times 10^{-6}$ °C^{-1}; $\theta_e = 80$ °C; $\theta_o = 25$ °C; $\nu = 0.35$; E = 70.0 MPa.

Herein, one comparison between numerical and experimental data of the dimensionless average moisture content and dimensionless surface temperature of the hollow brick obtained during the drying (T = 80 °C) are illustrate in Fig. 14. The mass transport coefficients (D and h_m) were estimated by using the least square error technique. The error and variance obtained for moisture content and temperature were $ERMQ_M = 0.259069$ (kg water/kg dry solid)^2 and $\overline{S}_M^2 = 0.181$ % kg water/kg dry solid and $ERMQ_T = 0.259069$ ($^oC/^oC$)^2 and $\overline{S}_T^2 = 0.181$ % °C/°C, respectively. The small error and variance indicates that the model presents good agreement with the experimental data. Some discrepancies appear at lowest moisture content and highest surface temperatures due to the fact that for longer drying

Table 2 Chemical composition of the clay (%)

SiO_2	Al_2O_3	Fe_2O_3	K_2O	MgO	CaO	TiO_2	SO_3	MnO	P_2O_5	ZrO_2	SrO	Rb_2O
57.054	24.25	9.257	2.879	2.789	2.049	1.259	0.149	0.140	0.071	0.048	0.034	0.021

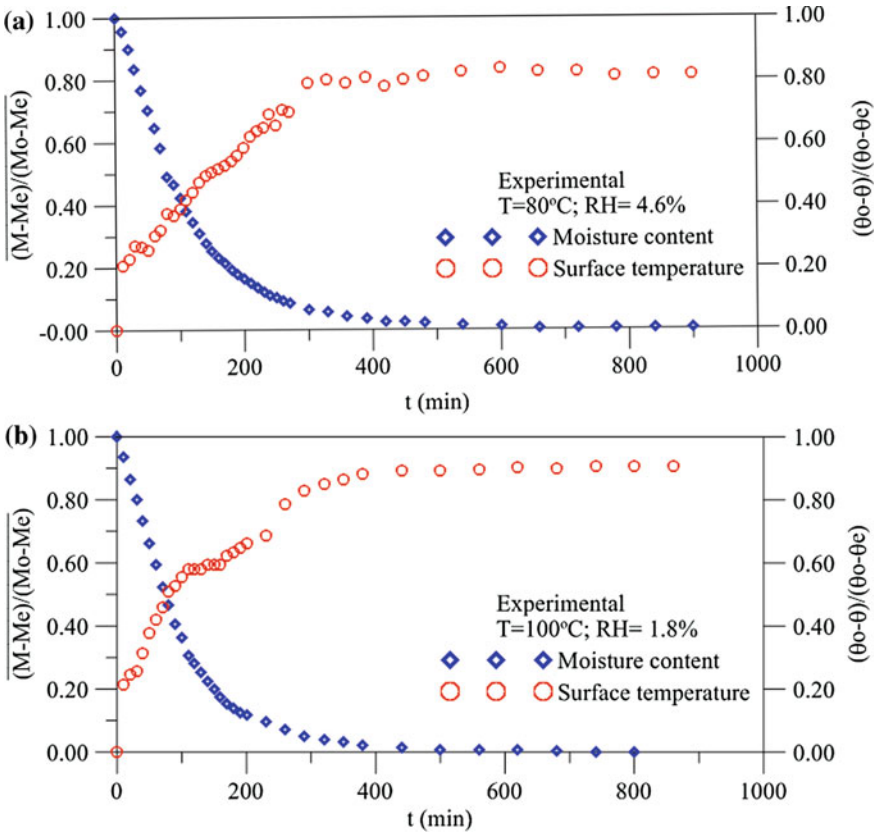

Fig. 7 Drying and heating kinetics of the industrial brick dried to the **a** T = 80 °C and **b** T = 100 °C

times the assumptions of constant thermal properties and polynomial shrinkage are probably not a good choice for this physical problem.

The drying parameters distributions inside the solid play important role to study the evolution of stresses, developed into the wet porous body during process. Then, moisture content, temperature and normal stresses distributions inside the solid obtained during drying ($z \cong R_3/2$) for elapsed times t = 300, 2000 and 8000 s are illustrate in Figs. 15, 16, 17. It is verified that highest moisture content and temperature gradients occurs at the surface of the solid mainly in the vertexes. So, these regions are more susceptible to cracks, fissures and deformations that reduce quality of the bricks.

It is verified that the drying induced stresses increased nonlinearly with the ΔM and $\Delta\theta$. The maximum stresses, therefore, may occur in the early stage of drying as low initial moisture content of the brick and when higher air temperature and lower relative humidity are used. In the beginning of the drying, because large

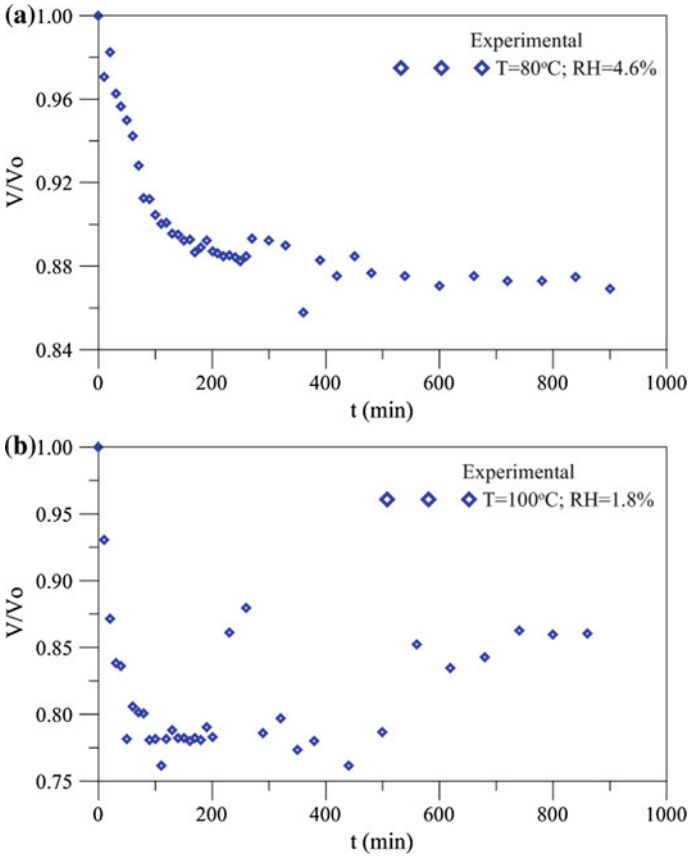

Fig. 8 Dimensionless volume of the clay brick as a function of drying time. **a** T = 80 °C and **b** T = 100 °C

temperature variations, the thermal stress are more than hydrical stress. For large elapsed time, both the hygro and thermal stresses vanish to equilibrium, and total stresses are of tensile in the center and surface. The maximum principal stress has occurred inside the hollow brick by combination of the heating and moisture migration effects.

According to literature [17], if the drying of molded clay is made to proceed too quickly, the result is that the surface dries up immediately while maintaining a wet state inside of product, the drying rate falls markedly and the product may develop cracks. Then, drying must be carried out very slowly under air controlled conditions (moderate temperature and high relative humidity) in order, to prevent undesirable cracks and deformations during the process and thus, obtaining product with good quality post-drying.

Research about strain and stress in clay during drying process has been reported in the literature [4, 14, 17, 36, 53, 54]. For common brick [4, 20, 53, 54], the

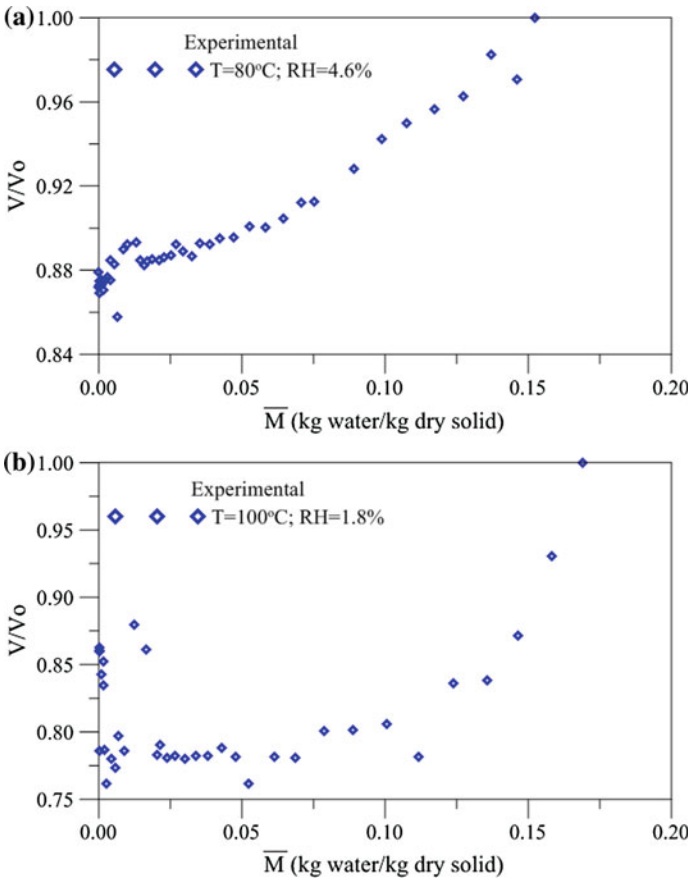

Fig. 9 Dimensionless volume of the clay brick as a function of the average moisture content. **a** T = 80 °C and **c** T = 100 °C

literature reports stress value at the external corner of approximately 0.45 MPa at the ended drying process. Obviously, this value depends on the brick material, process conformation, air and material conditions, etc. For comparison, at the equilibrium condition the maximum stresses values at the surface obtained here were $\sigma z = \sigma x = \sigma y = 1.105$ MPa.

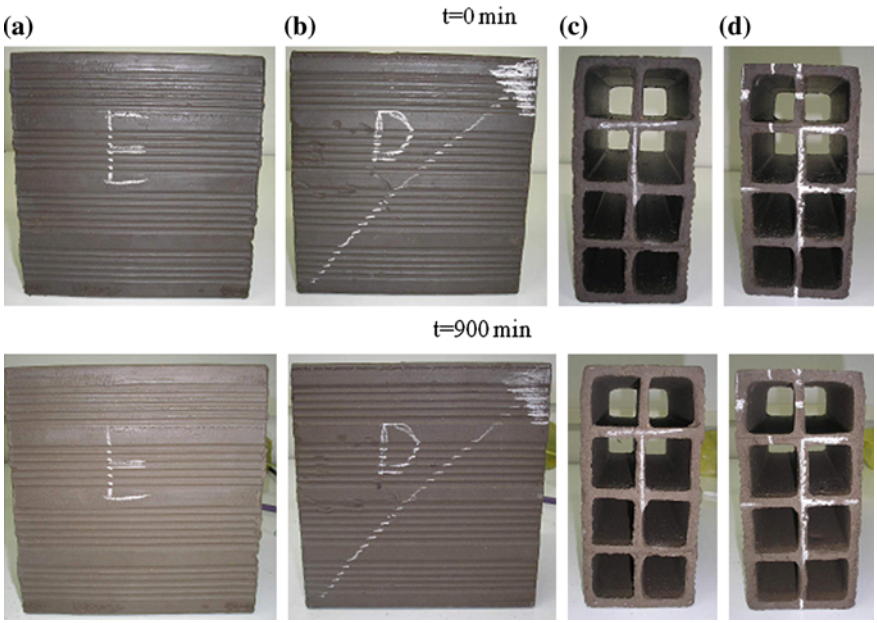

Fig. 10 View of the clay brick dried to the T = 80 °C. **a** *Left*, **b** *Right*, **c** *Back* and **d** *Front*

Fig. 11 View of the clay brick dried to the T = 80 °C

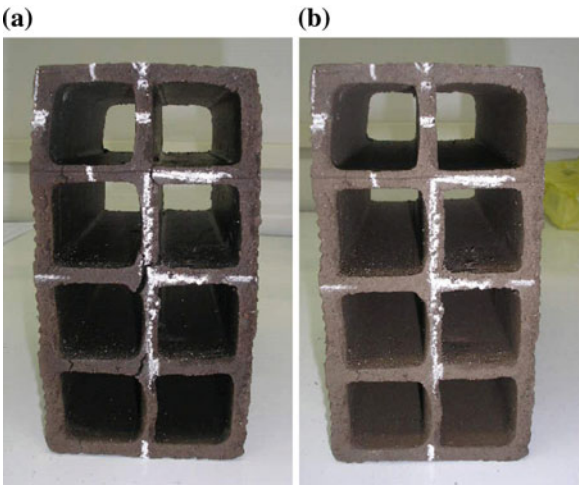

t = 40 min (θ_{brick} = 37.1°C) t = 900 min (θ_{brick} = 69.2°C)

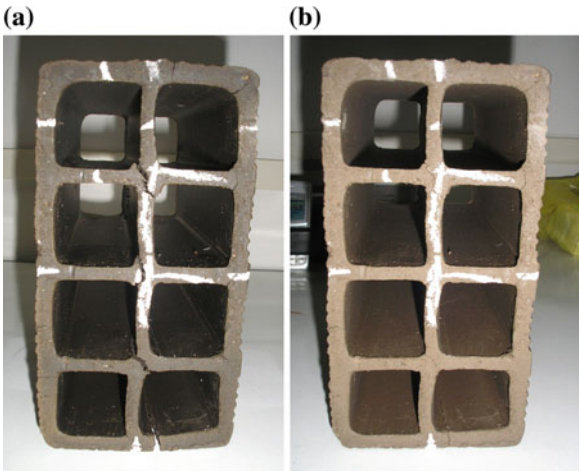

Fig. 12 View of the clay brick dried to the T = 90 °C

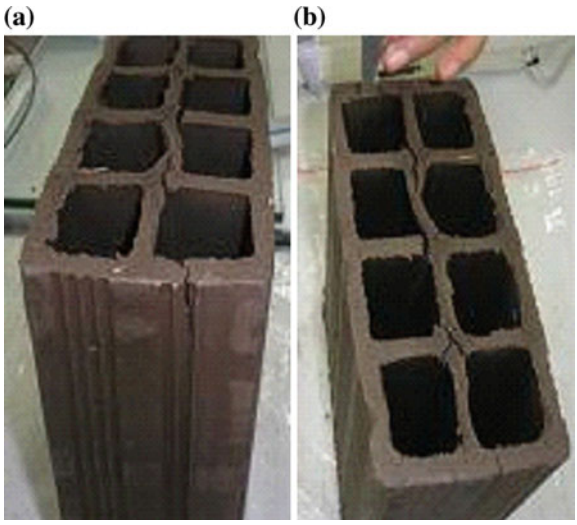

Fig. 13 View of the clay brick dried to the T = 100 °C in the elapsed time t = 40 min. **a** *Back* and **b** *Front*

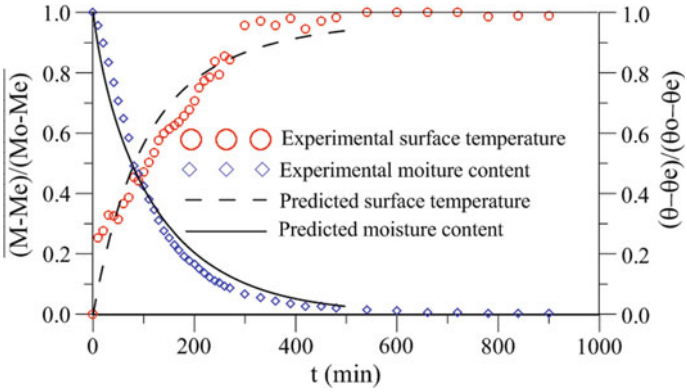

Fig. 14 Drying and heating kinetics of the industrial brick dried to T = 80 °C

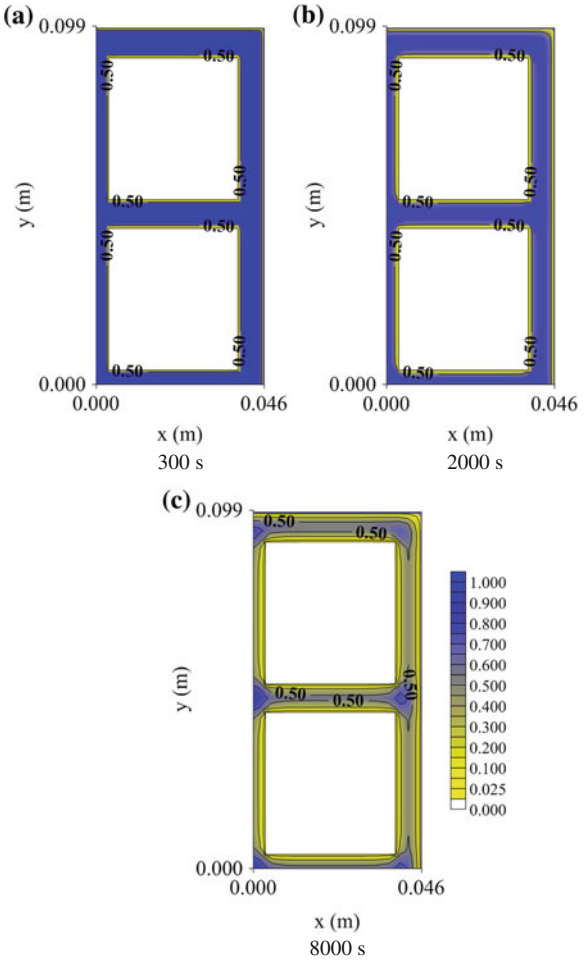

Fig. 15 Dimensionless moisture content [(M − Me)/(M_o − M_e)] at the xy plane (z = R_3/2)

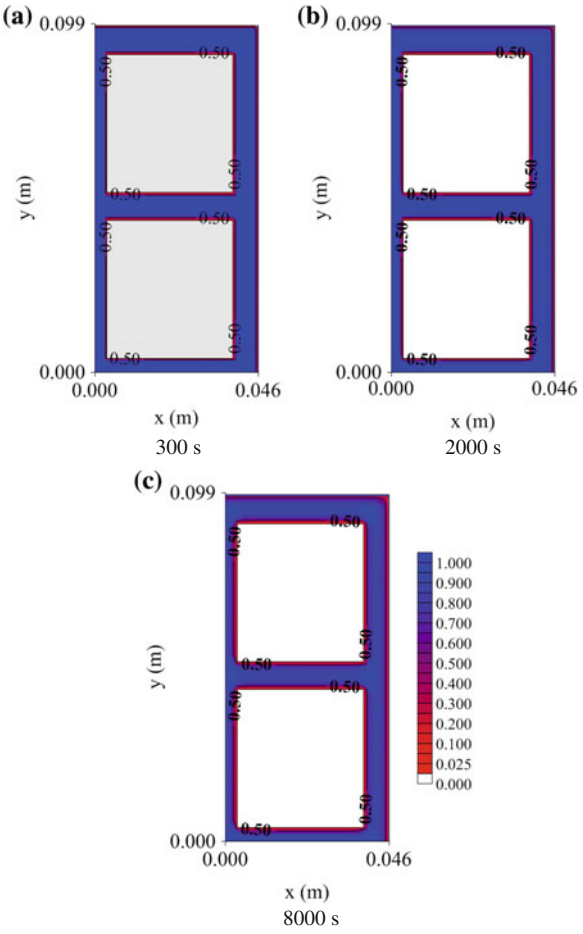

Fig. 16 Dimensionless temperature $[(\theta - \theta_e)/(\theta_o - \theta_e)]$ at the xy plane $(z = R_3/2)$

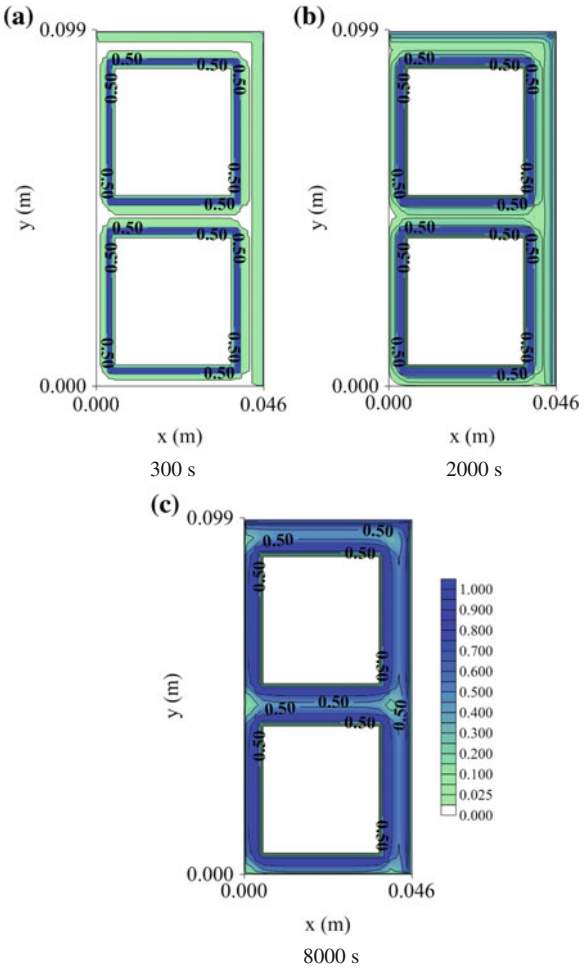

Fig. 17 Dimensionless principal stress $[(\sigma_z - \sigma_{min})/(\sigma_{max} - \sigma_{min})]$ at the xy plane ($z = R_3/2$). **a** $\sigma_{min} = 0$ and $\sigma_{max} = 1{,}103{,}471$ Pa, **b** $\sigma_{min} = 0$ and $\sigma_{max} = 1{,}103{,}473$ Pa and **c** $\sigma_{min} = 0$ and $\sigma_{max} = 1{,}103{,}473$ Pa

3 Concluding Remarks

In this chapter, a theoretical and experimental study has been presented. A three-dimensional mathematical modeling to predict heat transfer and moisture (liquid) migration in clay products with parallelepiped shape was developed, and the finite-volume method was employed to solve the governing equations. Formulation has been applied to predicted hollow brick drying process, and the stress and dimensions variations both induced by drying due to temperature and moisture changes has been investigated.

Based on the experimental results presented, the following conclusions can be summarized:

(a) The influence of temperature and relative humidity of the air as main factors in the drying rate is confirmed. As highest temperature and lowest relative humidity of the air are used in drying, heating and shrinkage rates will be higher, thus the total drying time becomes shorter.
(b) The areas near the internal and external surface (corner) of the brick present the largest rates of heat and mass transfer and largest volume variation and stresses, and so they are more susceptible areas to the cracks, fissures and deformations and even contribute to total fracture of the material;
(c) Stress due to moisture migration and high temperature can have a significant effect on the quality brick, mainly as high temperature and low relative humidity of the drying air are used.

The study indicates that the proposed modeling can be useful in:

(a) Good estimation of process time to dry the product;
(b) Reduction in energy consumption by allowing the detection of the correct processing time;
(c) Increased productivity of dried bricks, for allowing the withdrawal of the bricks from the dryer at the right time;
(d) Verification and understanding of the effect of process variables on product quality during drying and;
(e) Checking the appropriate process and dryer conditions, to improve product quality.

Acknowledgments The authors thank to FINEP, CAPES, CNPq and FACEPE (Brazilian Research Agencies) for financial support to this research, and also to the researchers for their referenced studies which helped in improving the quality of this work.

References

1. Callister Jr, W.D., Rethwisch, D.G.: Fundamentals of materials science and engineering: an integrated approach, 3rd edn. Wiley, New York (2008)
2. Callister Jr, W.D.: Materials science and engineering an introduction, 7th edn. Wiley, New York (2007)
3. Brosnan, D.A., Robinson, G.C.: Introduction to drying of ceramics. The American Ceramic Society, Westerville (2003)
4. Hasatani, M., Itaya, Y.: Modeling of strain-stress behavior for advanced drying. In: International Drying Symposium (Drying'96), vol. A, pp. 27–39. Krakow, Poland (1996)
5. Itaya, Y., Hasatani, M.: R & D needs-drying ceramics. Drying Technol. **14**(6), 1301–1313 (1996)
6. Reed, J.S.: Principles of ceramics processing. Wiley, New York (1995)
7. Sander, A., Skanki, D., Nenad, B.: Heat and mass transfer models in convective drying of clay slabs. Ceramics Inter. **29**, 641–643 (2003)
8. Ketelaars, A.A.J., Jomaa, W., Puiggali, J.R., Coumans, W.J.: Drying shrinkage and stress. In: International Drying Symposium (Drying'92), vol A, pp. 293–303 (1992)

9. Nascimento, J.J.S., Mederos, B.J.T., Belo, F.A., Lima, A.G.B.: Mass transport with shrinkage inside parallelepiped solids. Información Tecnológica **16**(1), 35–41 (2005). (In Spanish)
10. Nascimento, J.J.S., Lima, A.G.B., Teruel, B.J., Belo, F.A.: Heat and mass transfer with shrinkage during the ceramic bricks drying. Información Tecnológica **17**(6), 125–132 (2006). (In Spanish)
11. Silva, J.B., Almeida, G.S., Lima, W.C.P.B., Neves, G.A., Lima, A.G.B.: Heat and mass diffusion including shrinkage and hygrothermal stress during drying of holed ceramics bricks. Def. Diff. Forum **312–315**, 971–976 (2011)
12. Silva, W.P., Farias, V.S.O., Neves, G.A., Lima, A.G.B.: Modeling of water transport in roof tiles by removal of moisture at isothermal conditions. Heat Mass Transf. **48**(5), 809–821 (2012)
13. van der Zanden, A.J.J., Schoenmakers, A.M.E., Kerkof, P.J.A.M.: Isothermal vapour and liquid transport inside clay during drying. Drying Technol. **14**(3–4), 647–676 (1996)
14. Su, S.: Modeling of multi-phase moisture transfer and induced stress in drying clay brick. Appl. Clay Sci. **12**, 189–207 (1997)
15. van der Zanden, A.J.J.: Modelling and simulating simultaneous liquid and vapour transport in partially saturated porous materials. In: Mathematical Modeling and Numerical Techniques in Drying Technology. Marcel Dekker, Inc., New York (1997)
16. Itaya, Y., Taniguchi, S., Hasatani, M.: A Numerical study of transient deformation and stress behavior of a clay slab during drying. Drying Technol. **15**(1), 1–21 (1997)
17. Itaya, Y., Mori, S., Hasatani, M.: Effect of intermittent heating on drying-induced strain-stress of molded clay. In: International Drying Symposium (Drying'98), vol. A, pp. 240–247 (1998)
18. Augier, F., Coumans, W.J., A. Hugget, A., Kaasschieter, E.F.: On the risk of cracking in clay drying. In: International Drying Symposium (Drying'2000), CD ROM (2000)
19. Musielak, G.: Clay fracturing during drying. In: International Drying Symposium (Drying'2000), 1, CD ROM (2000)
20. Augier, F., Coumans, W.J., Hugget, A., Kaasschieter, E.F.: On the risk of cracking in clay drying. Chem. Eng. J. **86**, 133–138 (2002)
21. Banaszak, J., Kowalski, S.: Shrinkage and stress in viscoelastic cylinder in drying. In: International Drying Symposium (Drying'2000), 1, CD ROM (2000)
22. Kroes, B., Coumans, W.J., Kerkhof, P.J.A.M.: Drying behavior of deformable porous media: a mechanistic approach to clay drying. In: International Drying Symposium (Drying'96), vol. A, pp. 159–174. Krakow, Poland (1996)
23. Silva, J.B.: Simulation and Experimentation of the Drying of Drained Ceramic Bricks. Doctorate Thesis, Process Engineering, Federal University of Campina Grande, Paraíba, Brazil 174 (2009). (In Portuguese)
24. Almeida, G. S., Barbosa Fernandes, M.A.F., Ferreira Fernandes, J.N., G. Araújo Neves, G., Barbosa de Lima, W.M.P., Barbosa de Lima, A.G.B.: Drying of industrial ceramic bricks: An experimental investigation in oven. Def. Diff. Forum **353**, 116–120 (2014)
25. Silva, J.B., Almeida, G.S., Neves, G.A., Lima, W.C.P.B., Farias Neto, S.R., Lima, A.G.B.: Heat and mass transfer and volume variations during drying of industrial ceramic bricks: an experimental investigation. Def. Diff. Forum **326–328**, 267–272 (2012)
26. Almeida,G.S.: Simulation and experimentation of red ceramics drying in industrial thermal systems. Doctorate Thesis, Process Engineering, Federal University of Campina Grande, Paraíba, Brazil (2008). (In Portuguese)
27. Avelino, D.O., Nascimento, J.J.S., Lima, A.G.B., Simulation of the heat and mass transport during drying of holed ceramic bricks. In: 8o Congresso Iberoamericano de Engenharia Mecânica (CIBIM 2007), Cusco, Peru CD-ROM (2007). (In Portuguese)
28. Batista, V.R.J., Nascimento, J.S., Lima, A.G.B.: Drying and firing of common and holed ceramic bricks including dimensions variations and structural damages. Revista Eletrônica de Materiais e Processos **3**(1), 46–61 (2008). (In Portuguese)
29. Batista, V.R., Nascimento, J.J.S., Lima, A.G.B.: Drying and volumetric retraction of solid and hollow ceramic bricks: a theoretical and experimental investigation. Revista Matéria **14**(4), 1088–1100 (2009). (In Portuguese)

30. Nicolau, V.P., Lehmkuhl, W.A., Kawaguti, W.M., Dadam, A.P., Hartke, R.F., Jahn, T.G.: Numerical analysis of a continuous dryer used in red ceramic industry. In: III National Congress of Mechanical Engineering (CONEM 2004), pp. 1–10. Belém, Brazil (2004). (In Portuguese)
31. Santana, E.W.F.: Evaluation of drying and firing of ceramic plates. Master Dissertation in Science and Materials Engineering, Federal University of Campina Grande, Campina Grande, Brazil (2006). (In Portuguese)
32. Santos, G.M.: Study of thermal behavior of a tunnel kiln applied to red ceramic industry. Master Dissertation in Mechanical Engineering, Federal University of Santa Catarina, Florianópolis, Brazil (2001). (In Portuguese)
33. Nishikawa, T., Gao, T., Hibi, M., Takatsu, M., Ogawa, M.: Heat transmission during thermal shock testing of ceramics. J. Mater. Sci. **29**, 213–219 (1994)
34. Cadé, M.A., Nascimento, J.J.S., Lima, A.G.B.: Drying of holed ceramic bricks: an approach by finite-volumes. Revista Matéria **10**(3), 443–453 (2005). (In Portuguese)
35. Farias, V.S.O., Silva, W.P., Silva, C.M.D.P., Lima, A.G.B.: Three-dimensional diffusion in arbitrary domain using generalized coordinates for the boundary condition of the first kind: application in drying. Def. Diff. Forum **326–328**, 120–125 (2012)
36. Velthuis, J.F.M.: Simulation model for industrial dryers: reduction of drying times of ceramics & saving energy, In: International Drying Symposium (Drying'96), vol. B, pp. 1323–1328. Krakow, Poland (1996)
37. Recco, G.: Study to utilization of thermal energy from ceramic kiln to ceramic drying. Cerâmica Industrial **13**(3), 23–27 (2008). (In Portuguese)
38. Lehmkuhl, W.A.: Numerical and experimental analyses of a continuous dryer used in red ceramic industry. Master Dissertation in Mechanical Engineering, Federal University of de Santa Catarina, Florianópolis, Brazil (2004). (In Portuguese)
39. Hartke, R. F.: Numerical analysis of a continuous dryer used in red ceramic industry. In: 10th Brazilian Congress of Thermal Sciences and Engineering (ENCIT 2004), Rio de Janeiro, Brazil (2004). (In Portuguese)
40. Nicolau, V.P., Hartke, R.F., Jahn, T.G., Lehmkuhl, W.A.: Numerical and experimental analyses of a intermittent kiln to firing of ceramic products. In: National Congress of Mechanical Engineering (CONEM 2002), João Pessoa, pp. 1–10. Brazil (2002). (In Portuguese)
41. Almeida, G.S., Silva, J.B., Silva, C.J., Swarnakar, R., Neves, G.A., Lima, A.G.B.: Heat and mass transport in an industrial tunnel dryer: modeling and simulation applied to hollow bricks. Appl. Thermal Eng. **55**(1–2), 78–86 (2013)
42. Strumillo, C., Kudra, T.: Drying: principles, science and design. Gordon and Breach Science Publishers, New York (1986)
43. Brooker, D.B., Bakker-Arkema, F.W., Hall, C.W.: Drying and storage of grains and oilseeds. AVI Book, New York (1992)
44. Fortes, M., Okos, R.: Drying theories: their bases and limitations as applied to foods and grains . In: Mujumdar, A. (eds.) Advances in Drying. Hemisphere Publishing Corporation, Washington, vol. 1, pp. 119–154 (1980)
45. Keum, Y.T., Jeong, J.H., Auh, K.H.: Finite-element simulation of ceramic drying processes. Model. Simul. Mater. Sci. Eng. **8**, 541–556 (2000)
46. Keum, Y.T., Kim, J.H., Ghoo, B.Y.: Computer aided design of electric insulator. J. Ceramic Process. Res. **1**(1), 74–79 (2000)
47. Keum, Y.T., Oh, W.J.: Finite element simulation of a ceramic drying process considering pore shape and porosity. Model. Simul. Mater. Sci. Eng. **13**, 225–237 (2005)
48. Timoshenko, S.P., Goodier, J.N.: Theory of Elasticity. Guanabara Dois S.A., Rio de Janeiro (1980). (In portuguese)
49. Itaya, Y., Kobayashi, T., Hayakawa, K.: Three-dimensional heat and moisture transfer with viscoelastic strai-stress formation in composite food during drying. Int. J. Heat Mass Transf. **38**(7), 1173–1185 (1995)

50. Versteeg, H.K., Malalasekera, W.: An introduction to computational fluid dynamics: the finite method. Prentice Hall, London (1995)
51. Maliska, C.R.: Computational heat transfer and fluid mechanics. LTC-Livros Técnicos e Científicos Editora S.A, Rio de Janeiro (2004). (In Portuguese)
52. Patankar, S.V.: Numerical heat transfer and fluid flow. Hemisphere Publishing Corporation, New York (1980)
53. Hasatani, M., Itaya, Y.: Deformation characteristic of ceramics during drying. In: International Drying Symposium (Drying'92), vol. A, pp. 190–199. Montreal (1992a)
54. Hasatani, M., Itaya, Y.: Effect of drying process on quality control in ceramic production. In: International Drying Symposium (Drying'92), vol. B, pp. 1181–1198. Montreal (1992b)